PAPER

Simultaneously high thermal stability and low power based on Cu-doped GeTe phase change material

View the article online for updates and enhancements.

IOP ebooks™

Bringing you innovative digital publishing with leading voices to create your essential collection of books in STEM research.

Start exploring the collection - download the first chapter of every title for free.

Materials Research Express

PAPER

Simultaneously high thermal stability and low power based on Cu-doped GeTe phase change material

Yifeng Hu[1,3,4,5] , Tianshu Lai[2,5], Hua Zou[1] and Xiaoqin Zhu[2]

[1] School of Mathematics and Physics, Jiangsu University of Technology, Changzhou 213000, People's Republic of China
[2] State-Key Laboratory of Optoelectronic Materials and Technology, School of Physics, Sun Yat-Sen University, Guangzhou 510275, People's Republic of China
[3] State Key Laboratory of Silicon Materials, Zhejiang University, Hangzhou 310027, People's Republic of China
[4] Key Laboratory of Microelectronic Devices & Integrated Technology, Institute of Microelectronics, Chinese Academy of Sciences, Beijing 100029, People's Republic of China
[5] Authors to whom any correspondence should be addressed.

E-mail: hyf@jsut.edu.cn and stslts@mail.sysu.edu.cn

Abstract

The Cu-doped GeTe material was investigated systematically for its potential application in phase change memory. Compared with GeTe, $Ge_{40}Cu_{20}Te_{40}$ material had higher crystallization temperature (258 °C) and activation energy for crystallization (3.78 eV). After Cu adding, the band gap energy increased and the crystallization was restrained. A smoother surface for $Ge_{40}Cu_{20}Te_{40}$ material was achieved due to smaller grain size. The phase change memory device based on $Ge_{40}Cu_{20}Te_{40}$ material could have electrical switching with the RESET voltage of 2.65 V and pulse width 5 ns. The good thermal stability and low power demonstrated the promising application for Ge-Cu-Te material in phase change memory.

1. Introduction

With the explosive growth of information in the era of big data, it needs a great number of data memories. As the current mainstream memory, the NAND FLASH memory is faced with the limitation of continuous size minification as well as faster access speed due to its physical mechanism of charge storage [1, 2]. Phase change memory (PCM) is formed by a plurality of device cells having a chalcogenide region extending over an own heater. Driven by the Joule heating of current pulse, the chalcogenide can reversibly transform between an amorphous and a crystalline phase, resulting two vastly different resistance values to use as logic '0' and '1' storage states. More than 100 times faster to access than flash memory, PCM is a type of nonvolatile memory that has many possibilities for use as next-generation semiconductor memory [3]. What's more, the preferable scaling down in size make it possible to be applied for PCM in the smaller technology node and higher storage density.

As the core of PCM, phase change material has a significant effect on PCM. GeTe is a widely used phase change material because of its many advantages, such as fast phase change speed, stable chemical component and huge difference between the two resistance states (more than 5 orders of magnitude) [4, 5]. The structural properties of amorphous $GeTe_4$ are studied within the framework of first-principles molecular dynamics combined with density functional theory [6, 7]. However, the low crystallization temperature T_c (~180 °C) and associated poor data retention (~78 °C for ten years) make it insufficient in the future automobile electronic consumption which has a data retention requirement of above 120 °C [8]. Besides, the high RESET current is another main drawback to prevent its extensive use in high-density array. Doped GeTe material with N and O has been proved to have higher crystallization resistance and T_c by forming stronger Ge-N or Ge-O bonds. However, it is reported that the N [9] or O [10] doped GeTe materials undergo instability during the crystallization process due to the coexistence of atomic-state N (O) and molecular N_2 (O_2) in the crystalline materials. As is known, Sn [11] and Bi [12] doping can increase the crystallization speed of $Ge_2Sb_2Te_5$ and lower
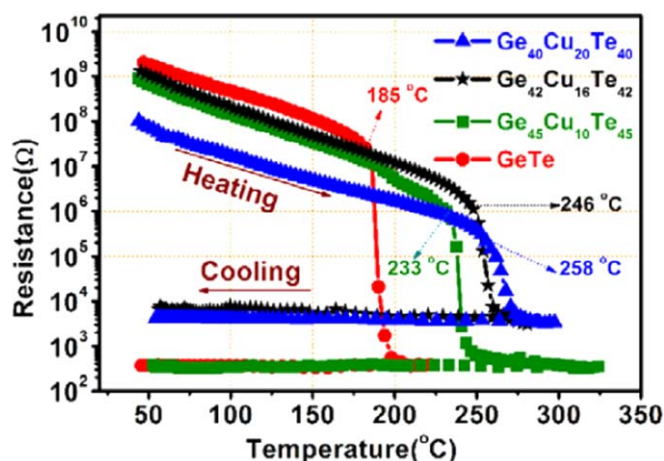
Figure 1. Resistance as a function of temperature at a heating rate and cooling rate of 5 °C min^{-1} for Ge-Cu-Te materials.

the melting temperature (T_m), however, lowering the T_c. Cu-doping can lower the T_m with the T_c also being increased, which is beneficial to lower the power and improve the thermal stability [13]. In this wok, Cu is used as a dopant to improve the performance of GeTe. A phase change material of Cu-doped GeTe was proposed for high data retention and low power for PCM application.

2. Experimental details

Ge-Cu-Te thin film materials were prepared on SiO_2/Si (100) substrates by co-sputtering Cu and GeTe targets at room temperature using magnetron sputtering system (JGP 450). For comparison, GeTe thin film was also fabricated by sputtering single GeTe target. The purity of the targets was more than 99.999 at% and the thickness of all materials was fixed at 50 nm by controlling the sputtering time. The thickness of all films were measured by the DEKTAK 6 M stylus profiler. The back ground pressure and work pressure of the sputtering system with gas Ar were 1.0×10^{-4} and 0.2 Pa, respectively. The sample pallets were kept rotating at a constant speed of 20 rpm to guarantee the homogeneity of composition. The sputtering power of Cu target was varied to obtain different content in Ge-Cu-Te films while the power of GeTe was immutably set at 15 W. The chemical composition of as-deposited Ge-Cu-Te materials were $Ge_{45}Cu_{10}Te_{45}$, $Ge_{42}Cu_{16}Te_{42}$ and $Ge_{40}Cu_{20}Te_{40}$ measured by energy dispersive x-ray spectroscopy (EDS, HITACHI, SU8010).

The resistance as a function of temperature ($R \sim T$) was measured *in situ* with a ramp rate of 5 °C min^{-1} in vacuum chamber by a Pt-100 thermocouple located at a heating stage controlled by a TP 94 temperature controller (Linkam Scientific Instruments Ltd, Surrey, UK). The 10-year data retention was estimated by recording the isothermal change in resistance with elevated temperature. The UV–vis-NIR spectrophotometer was used to measure the diffuse reflectivity spectra of the materials (7100CRT, XINMAO). The structure of the materials was characterized by x-ray diffraction (XRD, D/max2550VB3) with the diffraction angle range of 20 to 60°. X-ray photoelectron spectroscopy (XPS, Thermo ESCALAB 250XI) measurements with Al *Ka* radiation were employed to confirm the atomic percentage and the bonding situation of each element for GeTe and GeTeCu. The surface roughness of the materials was evaluated by atomic force microscopy (AFM, FM-Nanoview 1000), which was carried out in the semi-contact mode. The T-shaped PCM device cells with a 50 nm-thick thin film was fabricated using photolithography process, and then and ~200 nm Al top electrode was deposited above the phase change material in sequence. The PCM devices based on $Ge_{40}Cu_{20}Te_{40}$ materials were fabricated and the electrical switching property was measured by a Tektronix AWG5012B arbitrary waveform generator and a Keithley 2400 m.

3. Results and discussion

Figure 1 displays the resistance as a function of temperature in heating and cooling processes with a fixed rate of 5 °C min^{-1}. The tardy decreasing of material resistance is observed for all materials in initial heating process, which is ascribed to the negative temperature effect of semiconductor materials [14]. The temperature at which the resistance has an abrupt drop is defined as the crystallization temperature T_c. The thermal stability of amorphous material can be evaluated through the value of T_c. Figure 1 shows that the T_c for pure GeTe material
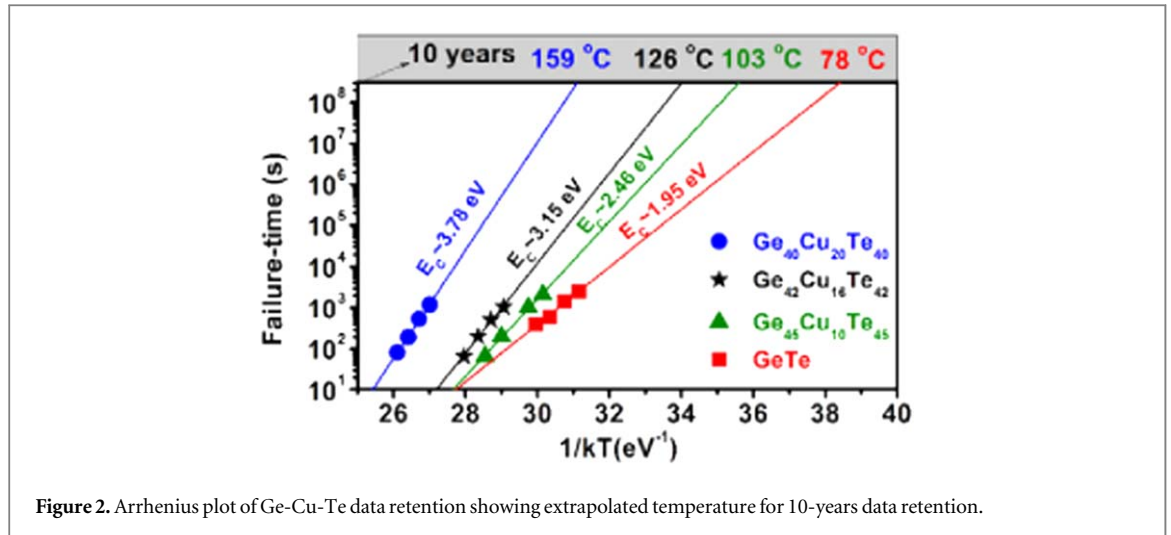
Figure 2. Arrhenius plot of Ge-Cu-Te data retention showing extrapolated temperature for 10-years data retention.

is about 185 °C, which is not enough to undergo the welding procedure involved in the assembling process between chips and printed circuit board (at least 220 °C for 1 min) [4]. After Cu doping, the T_c increases to higher values (233 °C for $Ge_{45}Cu_{10}Te_{45}$, 246 °C for $Ge_{42}Cu_{16}Te_{42}$, 258 °C for $Ge_{40}Cu_{20}Te_{40}$), indicating the thermal stability is enhanced by Cu adding. In the subsequent cooling process, the resistance of all materials maintains low values, which further confirms the transformation of amorphous-to-crystalline state. The resistance change for $Ge_{40}Cu_{20}Te_{40}$ material approaches to two orders of magnitude, which is enough for sufficient signal-to-noise ratio. In addition, the crystallization resistance has been improved from 330 Ω of GeTe to 4282 Ω of $Ge_{40}Cu_{20}Te_{40}$. In PCM device cells, the resistance switching is achieved by absorbing the Joule heating of current pulse. According to the Joule heat equation: $E = I^2 \cdot R \cdot t$, where E, I, R, t are heat, electricity, resistance and time respectively (with the units J, A, Ω and s), a bigger resistance value can improve the self-heating efficiency, resulting a lower power consumption in RESET operation.

In order to further evaluate the data retention of phase change materials, the isothermal crystallization was carried out for all materials. Before T_c, four temperatures with the fixed interval of 5 °C were selected as isothermal temperature. With annealing time increasing, the resistance of phase change materials decreases gradually due to energy accumulation. In this work, the time when the resistance drops to 50% of its initial value is regarded as the failure time. The plot of logarithm failure time versus $1/kT$ is shown in figure 2. The fitted straight line, fitting a linear Arrhenius relationship due to its thermal activation nature, can be described as [15]:

$$t = \tau_0 \exp\left(E_c / k_b T\right) \qquad (1)$$

where t, τ_0, E_c, k_b, T are the failure time, pre-exponential factor associated with the material's properties, activation energy for crystallization, Boltzmann's constant and absolute temperature of concern, respectively. The E_c, in connection with the difficult for crystallization, increases from 1.95 eV of GeTe to 3.78 eV of $Ge_{40}Cu_{20}Te_{40}$. Accordingly, the holding temperature for 10 years obtained by extrapolating the fitted straight line are 78, 103, 126 and 159 °C for GeTe, $Ge_{45}Cu_{10}Te_{45}$, $Ge_{42}Cu_{16}Te_{42}$, $Ge_{40}Cu_{20}Te_{40}$, respectively. Obviously, the data retention has been greatly improved by Cu doping, which is in accord with the results in figure 1.

The diffuse reflectivity spectra of Ge-Cu-Te were measured at room temperature ranging from 400 to 2500 nm. By extrapolating the absorption edge onto the energy axis in figure 3, the band gap energy (E_g) can be determined. The Kubelka-Munk function (K-M) is used for the conversion of the reflectivity to absorbance data [16]:

$$\frac{K}{S} = \frac{(1 - R)^2}{2R} \qquad (2)$$

where K, S and R represent the absorption coefficient, scattering coefficient and reflectivity, respectively. In semiconductor materials, the carrier concentration can be obtained through the relationship [17]: $n^2 = CT^3 \exp\left(-\frac{E_g}{kT}\right)$, where n is carrier concentration, C is constant, T is absolute temperature and k is Boltzmann's constant. A higher E_g can result in higher carrier concentration as well as lower resistivity. For as-deposited $Ge_{40}Cu_{20}Te_{40}$ material, the E_g is 1.33 eV. After annealed at 300 °C for 10 min, the E_g decreases to 1.22 eV. Besides, the annealed GeTe has lower E_g of 0.71 eV. The trend is proportional to that of resistance in figure 1.

The phase structure of GeTe and $Ge_{40}Cu_{20}Te_{40}$ materials are analyzed by XRD as shown in figure 4. In as-deposited and 150 °C annealed GeTe materials, no diffraction peaks are observed, indicating the amorphous structure. When the annealing temperature exceeds 240 °C, the three diffraction peaks (111), (200) and (220)
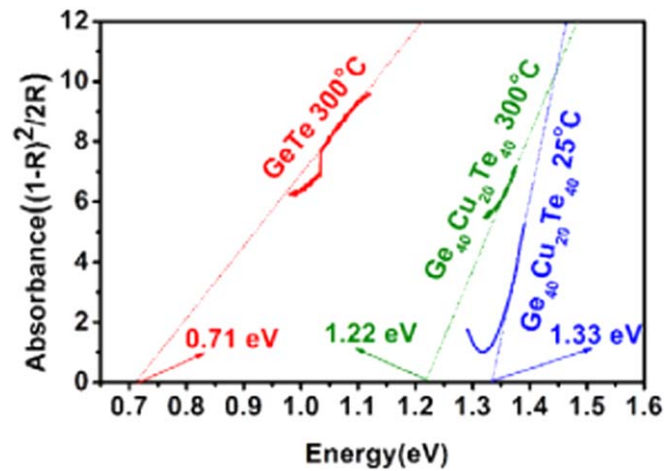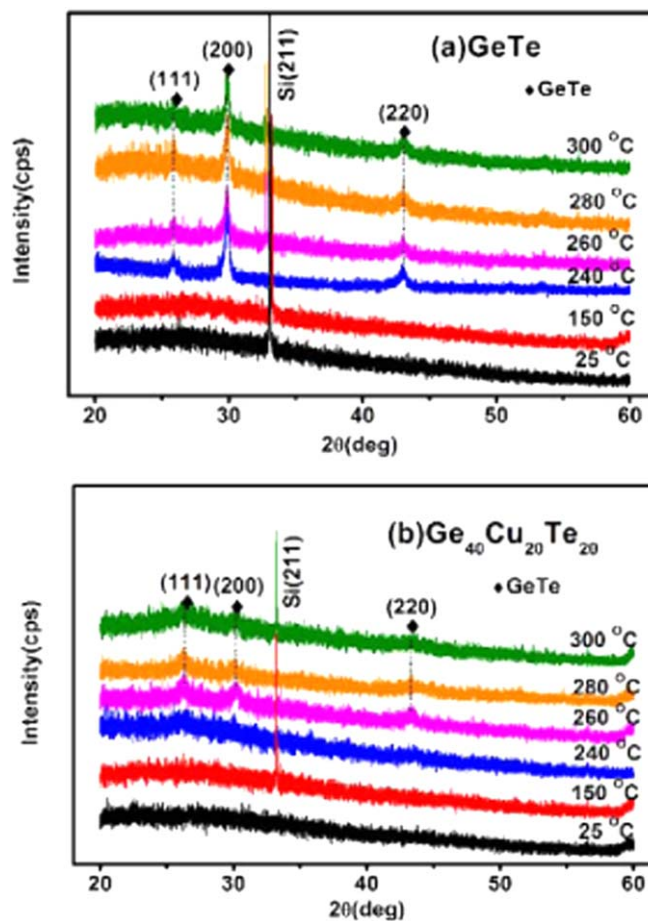
Figure 3. The Kubelka-Munk function of GeTe and $Ge_{40}Cu_{20}Te_{40}$ materials.

Figure 4. XRD patterns of (a) GeTe, (b) $Ge_{40}Cu_{20}Te_{40}$ materials annealed at different temperatures for 10 min in Ar atmosphere.

appear, belonging to the characteristic GeTe phase. Unlike GeTe, no obvious diffraction peaks are found for $Ge_{40}Cu_{20}Te_{40}$ materials below 240 °C, exhibiting a better thermal stability than GeTe. Except the same three diffraction peaks as GeTe material, no new diffraction peaks are observed for $Ge_{40}Cu_{20}Te_{40}$ material even after annealing at 300 °C. It shows that no new phase containing Cu element forms. From the main peak at around 29.9°, the grain sizes of annealed GeTe and $Ge_{40}Cu_{20}Te_{40}$ materials are 25.3 and 18.2 nm, respectively, calculated using the Scherrer equation ($D_{hkl} = 0.943\lambda/\beta \cos\theta$). It can be infered that the doped Cu maybe exist

The surface bonding states of the materials are studied by XPS. The Ge 2p peaks at 1220.0 and 1251.4 eV represent Ge-Te bonds in GeTe material [18]. As shown in figure 5(a), the same peaks belonging to Ge 2p are
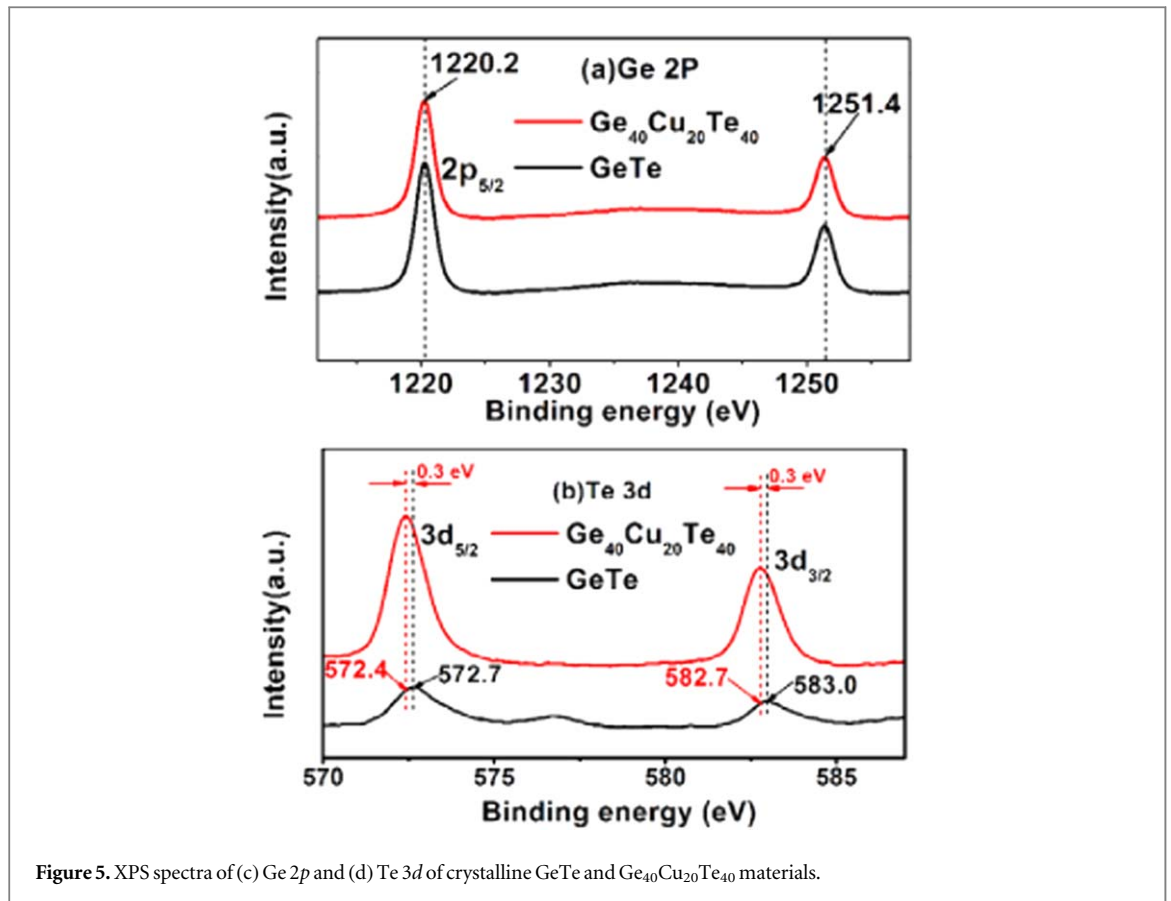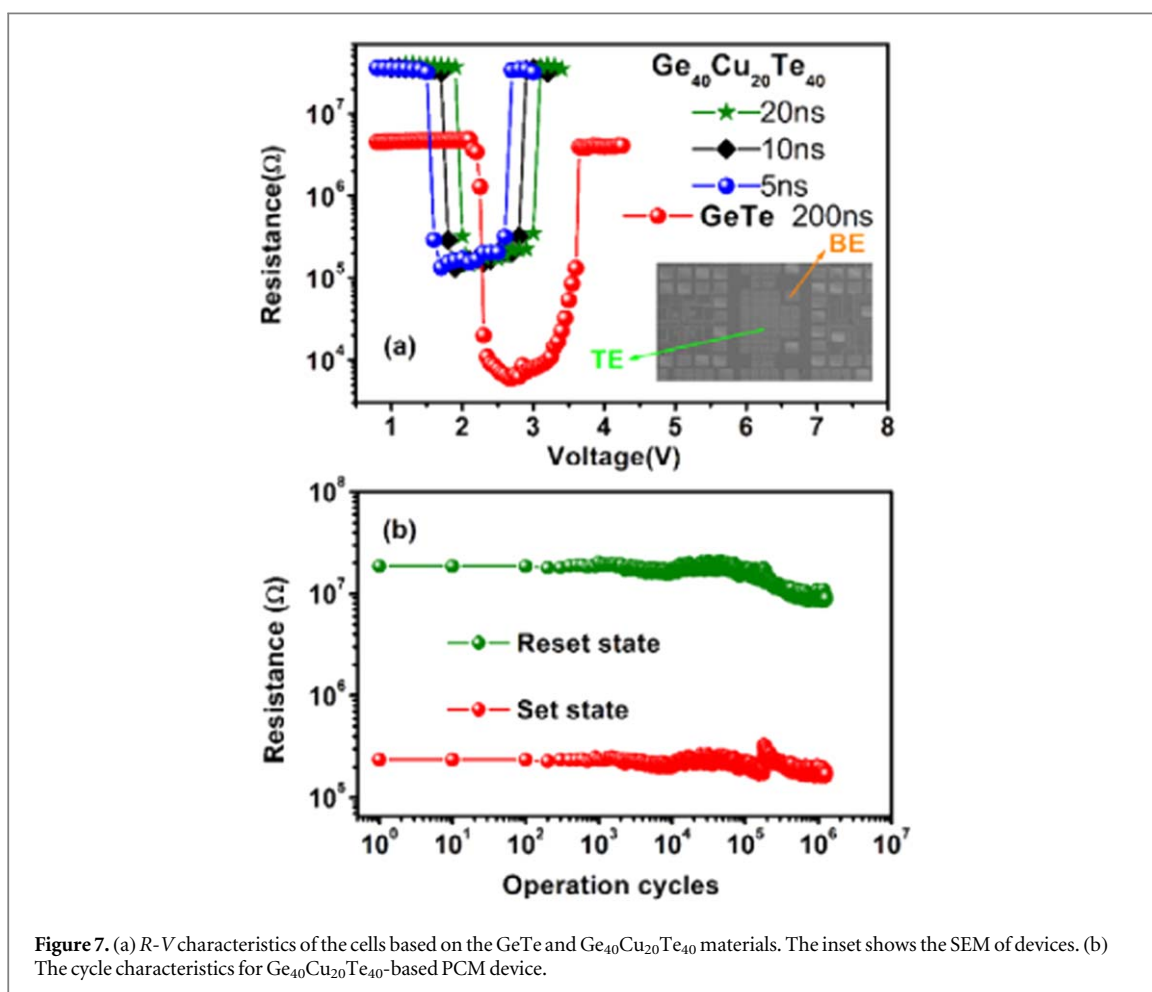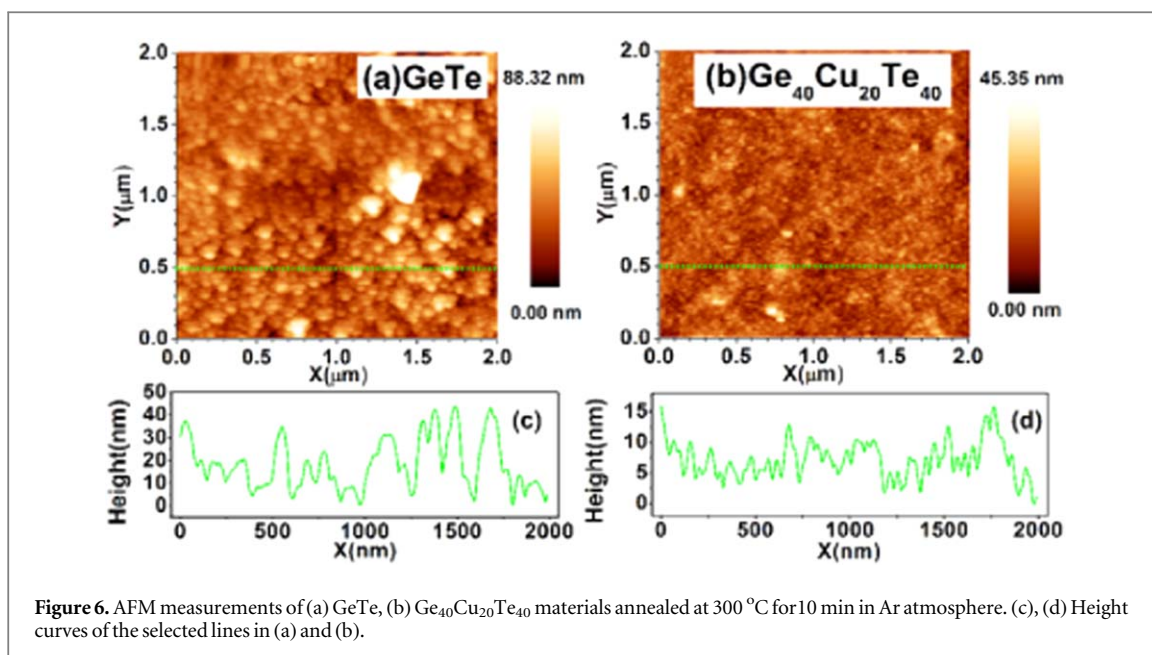
Figure 5. XPS spectra of (c) Ge 2*p* and (d) Te 3*d* of crystalline GeTe and Ge₄₀Cu₂₀Te₄₀ materials.

observed for $Ge_{40}Cu_{20}Te_{40}$ material, indicating no new bonds generate between Ge and Cu atoms. Unlike the Ge atoms, the shift of Te 3d peaks are displayed in figure 5(b). The peaks of Te 3d5/2 and 3d3/2 locate at 572.7 and 583.0 eV, respectively. After Cu doping, a 0.3 eV shift toward low energy is detected for $Ge_{40}Cu_{20}Te_{40}$ material. The atomic radius for Cu, Ge and Te atoms are 1.28, 1.40 and 1.70 Å, respectively. That is, the Cu atom is smaller than Ge and Te atoms. When Cu doping, the Cu atoms can enter into the GeTe lattice, resulting in the lattice distortion. It may cause the shift of peak.

The morphology of phase change material, associated with the crystallization process, is significant to the high cycling of the read and write operations in PCM device. Figure 6 shows the AFM results of annealed GeTe and $Ge_{40}Cu_{20}Te_{40}$ materials at 300 °C for 10 min in Ar atmosphere with the scanned areas of 2 μm. A great deal of crystal particles can be observed in the surface of GeTe and $Ge_{40}Cu_{20}Te_{40}$ materials, indicating the formation of crystallization state. Compared with GeTe, the crystal particles of $Ge_{40}Cu_{20}Te_{40}$ materials are more compact and homogeneous. In order to further evaluate the grain size quantificationally, the line scanning is made with the location of green lines in figures 6(a) and (b). The corresponding height curves of the selected lines are shown in figures 6(c) and (d). The density of fluctuant peaks for GeTe is sparser than $Ge_{40}Cu_{20}Te_{40}$ materials. The results display that the root-mean-square surface roughness for $Ge_{40}Cu_{20}Te_{40}$ is 1.8652 nm, which is much smaller than that of GeTe (12.6534 nm). The smooth surface in Cu-doped GeTe material indicates that Cu dopant can restrain the grain growth, leading to smaller grain size and better interfacial contact of electrode-film.

The PCM device based on $Ge_{40}Cu_{20}Te_{40}$ material are fabricated by 0.18-μm complementary metal-oxide semiconductor (CMOS) technology to examine the electrically induced switching characteristics. The scanning electron microscope of the device cells is shown in the inset of figure 7(a). Several top electrodes (TE) have a common bottom electrode (BE). The pulse currents of different time width are applied in TE and BE. Between the phase change material and electrode, 20-nm TiN is deposited to increase the adhesiveness. The integrated SET and RESET operation can be achieved for $Ge_{40}Cu_{20}Te_{40}$ by applying the voltage pulses of 20, 10 and 5 ns width. The resistance change exceeds two orders of magnitude. The lowest RESET voltage for $Ge_{40}Cu_{20}Te_{40}$ is 2.65 V, which is much lower than that of GeTe (3.82 V). Besides, the pulse width 5 ns for $Ge_{40}Cu_{20}Te_{40}$ is shorter than GeTe (200 ns), indicating a faster switching speed for $Ge_{40}Cu_{20}Te_{40}$. The necessary energy for RESET operation E_{reset} can be estimated by $(V_{reset}^2/R_{reset}) \times t_{reset}$. The energy for the RESET operation of $Ge_{40}Cu_{20}Te_{40}$ cell is calculated to be around 3.4×10^{-13} J, which is approximately three orders of magnitude lower than that of GeTe cell (6.8×10^{-10} J). The results show that $Ge_{40}Cu_{20}Te_{40}$-based PCM device has a lower power consumption and faster storage speed than GeTe. The endurance cycling characteristics of PCM devices are

Figure 6. AFM measurements of (a) GeTe, (b) $Ge_{40}Cu_{20}Te_{40}$ materials annealed at 300 °C for 10 min in Ar atmosphere. (c), (d) Height curves of the selected lines in (a) and (b).

Figure 7. (a) *R-V* characteristics of the cells based on the GeTe and $Ge_{40}Cu_{20}Te_{40}$ materials. The inset shows the SEM of devices. (b) The cycle characteristics for $Ge_{40}Cu_{20}Te_{40}$-based PCM device.

shown in figure 7(b). The 200 ns pulses rated at 2.2 and 3.5 V are alternately applied for SET and RESET operations, respectively. A reversible switching up to 1.0×10^6 cycles without failure is achieved. The good endurance character demonstrates the practicability of $Ge_{40}Cu_{20}Te_{40}$ materials.

4. Conclusion

In summary, Ge-Cu-Te materials are prepared by adding Cu into GeTe. After Cu-doping, the T_c increases from 185 ^{o}C of GeTe to 258 ^{o}C of Ge$_{40}$Cu$_{20}$Te$_{40}$. According to the extrapolated data, Ge$_{40}$Cu$_{20}$Te$_{40}$ material has good data retention (159 ^{o}C for 10 years). The crystal Ge$_{40}$Cu$_{20}$Te$_{40}$ material has broader band gap (1.22 eV) than GeTe (0.71 eV). No new phases are observed in Ge$_{40}$Cu$_{20}$Te$_{40}$ material. A smoother surface for Ge$_{40}$Cu$_{20}$Te$_{40}$ is achieved with the root-mean-square surface roughness of 1.8652 nm. A lower RESET operation voltage (2.65 V) and a faster switching speed (5 ns) are realized for Ge$_{40}$Cu$_{20}$Te$_{40}$-based PCM device. A good endurance character is demonstrated by the 1.0×10^6 cycles without failure. Ge-Cu-Te material is a promising phase change material to have good thermal stability and low operation power.

Acknowledgments

ORCID iDs

Yifeng Hu ● https://orcid.org/0000-0001-7088-6829

References

[1] Wu W H, Zhao Z H, Shen B, Zhai J W, Song S N and Song Z T 2018 *Nanoscale* **10** 7228
[2] Wang Z R *et al* 2017 *Nat. Mater.* **16** 101
[3] Rao F *et al* 2017 *Science* **358** 1423
[4] Hwang I, Cho Y J, Lee M J and Jo M H 2015 *Appl. Phys. Lett.* **106** 193106
[5] Sa B S, Zhou J, Sun Z M, Tominaga J and Ahuja R 2012 *Phys. Rev. Lett.* **109** 096802
[6] Bouzid A, Massobrio C, Boero M, Ori G, Sykina K and Furet E 2015 *Phys. Rev.* B **92** 134208
[7] Bouzid A, Zaoui H, Palla P L, Ori G, Boero M, Massobrio C, Clerib F and Lampin E 2017 *Phys. Chem. Chem. Phys.* **19** 9729
[8] Morikawa T, Kurotsuchi K, Fujisaki Y, Matsui Y and Takaura N 2012 *Jpn. J. Appl. Phys.* **51** 031201
[9] Kolobov A V, Fons P, Hyot B, Andre B, Tominaga J, Tamenori Y, Yoshikawa H and Kobayashi K 2012 *Appl. Phys. Lett.* **100** 061910
[10] Linggang Z, Zhen L, Jian Z, Naihua M and Zhimei S 2017 *J. Mater. Chem.* C **5** 3592
[11] Fernandes B J, Naresh N, Ramesh K, Sridharan K and Udayashankar N K 2017 *J. Alloy. Compd.* **721** 674
[12] Yang T Y, Cho J Y, Park Y J and Joo Y C 2012 *Acta Mater.* **60** 2021
[13] Ding K Y, Ren K, Rao F, Song Z T, Wu L C, Liu B and Feng S L 2014 *Mater. Lett.* **125** 143
[14] Hua Z, Hu Y F, Zhu X Q, Sun Y M, Zheng L, Sui Y X, Wu S C and Song Z T 2017 *J. Mater. Sci.* **52** 5216
[15] Hu Y F, Zhu X Q, Zou H, You H P, Shen D H, Song S N and Song Z T 2017 *J. Alloy. Compd.* **727** 986
[16] Hu Y F, Zhu X Q, Zou H, Zhang J H, Yuan L, Xue J Z, Sui Y X, Wu W H, Song S N and Song Z T 2016 *Appl. Phys. Lett.* **108** 223103
[17] Rao F, Song Z T, Cheng Y, Xia M J, Ren K, Wu L C, Liu B and Feng S L 2012 *Acta Mater.* **60** 323
[18] Vinod E M, Singh A K, Ganesan R and Sangunni K S 2012 *J. Alloy. Compd.* **537** 127